

# An anti-C3b(i) mAb enhances complement activation, C3b(i) deposition, and killing of CD20<sup>+</sup> cells by rituximab

Adam D. Kennedy, Michael D. Solga, Theodore A. Schuman, Amos W. Chi, Margaret A. Lindorfer, William M. Sutherland, Patricia L. Foley, and Ronald P. Taylor

**We investigated deposition of the complement protein fragment C3b and its breakdown products (collectively designated as C3b(i)) on CD20-positive cells treated with rituximab (RTX) in the presence of normal human serum (NHS). Radioimmunoassay (RIA) demonstrates that about 500 000 C3b(i) molecules deposit per cell, and fluorescence microscopy reveals that C3b(i) colocalizes with bound RTX. Use of mAb 3E7, specific for C3b(i) bound to substrates, enhances C3b(i) deposition; > 1 million C3b(i) deposit when cells are incubated with NHS, RTX and mAb 3E7.**

**Treatment of Raji cells in NHS plus RTX leads to robust cell killing (95%) after 24 to 48 hours, and mAb 3E7 significantly enhances RTX-mediated killing of Raji and DB cells. A cynomolgus monkey model based on intravenous infusion of RTX followed by mAb 3E7 demonstrated that RTX rapidly binds to B cells and promotes complement activation and C3b(i) deposition; fluorescence microscopy analyses revealed the same pattern of colocalization of C3b(i) on cell-bound RTX in vivo as observed in vitro. Preliminary in vitro studies with blood samples**

**from patients with chronic lymphocytic leukemia lead to similar findings. These experiments suggest that complement plays a key role in the mechanism of action of RTX; moreover, the in vivo molecular form of RTX (and possibly other antitumor mAbs) in the circulation or in tissues may include C3b(i) molecules covalently bound to the therapeutic mAb, thus allowing it to interact with cells containing both Fc and complement receptors. (Blood. 2003;101:1071-1079)**

© 2003 by The American Society of Hematology

## Introduction

Deposition of nascent C3b on cell surfaces during complement (C) activation can opsonize cells for destruction.<sup>1-4</sup> Cancer cells can activate the alternative or classical C pathway, which results in the covalent attachment of C3b molecules, thus perpetuating C activation and promoting cell lysis.<sup>5-8</sup> Cell-bound C3b can be degraded to inactive forms, iC3b and then C3dg, by C control proteins on these cells, which effectively stops C activation; in fact, C control proteins may protect malignant cells from C-mediated destruction.<sup>9,10</sup> We proposed, however, that it may be possible to target cancer cells by using monoclonal antibodies (mAbs) specific for the residual cell-bound C3b(i).<sup>5</sup> The murine mAb 3E7 shows enhanced specificity for C3b(i) covalently attached to a cell surface, and it can bind to C3b(i)-opsonized cells in whole blood in the presence of solution phase C3b(i). As with any tumor-specific antigen, the level of C3b(i) available on cancer cells is critical to such an immunotherapeutic approach. Deposition of C3b(i) on cancer cells due to naturally occurring complement activation may not provide sufficient C3b(i) for such targeting, even with a high avidity and specific anti-C3b(i) mAb such as 3E7.<sup>11-13</sup>

The anti-CD20 mAb rituximab (RTX) has proven effective in treating B-cell malignancies.<sup>14-20</sup> Although the mechanism of action of RTX in vivo has not been clearly elucidated,<sup>21-27</sup> RTX activates C when it binds to CD20<sup>+</sup> B cells and it can promote C-mediated lysis of targeted cells.<sup>28-37</sup> We reasoned that in the

presence of C, RTX might facilitate deposition of large amounts of C3b(i) on CD20<sup>+</sup> B cells, and that mAb 3E7 might be useful in examining and perhaps enhancing this process as well as in augmenting RTX/C-mediated cell lysis. We have used flow cytometry, radioimmunoassay (RIA), steady state fluorescence measurements, and fluorescence microscopy to test these hypotheses.

## Materials and methods

### Cell lines, sera, and plasmas

ARH-77, DB, GA-10, Raji, and Ramos cells were obtained from American Type Culture Collection (ATCC, Manassas, VA) and maintained in log phase growth at 37°C in 5% CO<sub>2</sub> in complete media (RPMI 1640; ATCC) supplemented with 10% fetal bovine serum and penicillin/streptomycin (Gibco BRL, Grand Island, NY). Cells were pelleted at 450g for 3 minutes and suspended in fresh complete medium. Viability defined by trypan blue exclusion was more than 95%. GA-10 and Ramos cells were rapidly killed by RTX in 50% normal human serum (NHS; not shown), and these cells were not used further in killing assays. For certain experiments ARH-77 cells were labeled with PKH26 (Sigma, St Louis, MO) according to the manufacturer's directions. Blood was obtained, with informed consent according to the Declaration of Helsinki, from healthy volunteers or from patients with chronic lymphocytic leukemia (CLL). The University of Virginia institutional review board approved this study. NHS and citrated

From the Department of Biochemistry and Molecular Genetics, the Department of Cell Biology, and the Center for Comparative Medicine, University of Virginia Health Sciences Center, Charlottesville.

Submitted March 20, 2002; accepted August 27, 2002. Prepublished online as *Blood* First Edition Paper, September 5, 2002; DOI 10.1182/blood-2002-03-0876.

Supported by funding from EluSys Therapeutics Inc, Pine Brook, NJ (R.P.T., M.A.L., W.M.S.).

Two of the authors (R.P.T., W.M.S.) have declared a financial interest in a company whose potential product was studied in the present work.

**Reprints:** Ronald P. Taylor, Box 800733, University of Virginia Health Sciences Center, Charlottesville, VA 22908-0733; e-mail: rpt@virginia.edu.

The publication costs of this article were defrayed in part by page charge payment. Therefore, and solely to indicate this fact, this article is hereby marked "advertisement" in accordance with 18 U.S.C. section 1734.

© 2003 by The American Society of Hematology

plasmas were processed within 1 hour of collection and stored at  $-80^{\circ}\text{C}$ . Baby rabbit complement (BRC) was obtained from Cedarlane Laboratories (Hornby, ON, Canada).

### Monoclonal antibodies

IgG1 mAbs 7C12 and 3E7, specific for C3b(i), and IgG1 mAb HB43, specific for human IgG, have been described.<sup>5,38,39</sup> RTX (IDEC Pharmaceuticals, San Diego, CA) was purchased at the University of Virginia (UVA) pharmacy and the hybridoma for anti-CD20 mAb 1F5 (HB9645) was obtained from ATCC. MAbs were labeled with  $^{125}\text{I}$  (Iodogen; Pierce, Rockford, IL),<sup>39,40</sup> with fluorescein isothiocyanate (FITC),<sup>41</sup> with Alexa dyes (Molecular Probes, Eugene, OR), or with phycoerythrin (PE; Prozyme, San Leandro, CA) according to the manufacturers' directions. MAbs specific for epitopes expressed on B cells were as follows (epitopes identified first): CD19, IgG1, SJ25-C1 (Caltag, Burlingame, CA); CD21, IgG2a, HB135 (ATCC); CD22, IgG1 RFB4 (Caltag); CD32, IgG2b, HB217 (ATCC); CD55, IgG1, 67 (Serotech, Oxford, United Kingdom); CD59, rat IgG2b, YTH 53.1 (Serotech); rat IgG2b isotype control, MCA1125 (Serotech).

### Opsonization of cells

**Flow cytometry.** Raji or ARH-77 cells in complete medium ( $1 \times 10^5$  to  $2 \times 10^6$  cells/mL) were mixed with an equal volume of NHS or citrated plasma, or ethylenediamine tetraacetic acid (EDTA)-plasma, and then RTX  $\pm$  mAb 3E7 were added to final concentrations of  $10 \mu\text{g/mL}$ . In all experiments that made use of human serum or plasmas for opsonization or for tests of RTX-mediated killing, the concentration of NHS, citrated plasma, or EDTA-plasma was 50% by volume. After incubation for 30 minutes at  $37^{\circ}\text{C}$ , cells were washed twice with 1% bovine serum albumin in phosphate buffered saline (BSA-PBS) and developed with FITC mAb 7C12 and PE mAb HB43. Alternatively, the cells were opsonized in NHS with Alexa 633 RTX and Alexa 488 mAb 3E7 at  $10 \mu\text{g/mL}$  each.

**RIA.** Similar protocols were followed, using  $^{125}\text{I}$ -labeled RTX or mAb 3E7, and molecules bound per cell were determined after 3 washes in BSA-PBS. In indirect RIA, cells were first incubated with unlabeled mAbs, and after 3 washes, saturating amounts of  $^{125}\text{I}$  mAb HB43 or mAb 7C12 were added. Duplicate aliquots were spun through oil after 30 minutes' incubation at room temperature and pelleted radioactivity was used to calculate molecules of cell-bound RTX and C3b(i), respectively.<sup>39</sup> All statistical analyses for these and other experiments were based on *t* tests using Sigma Stat (Jandel, San Rafael, CA).

**Steady state fluorescence.** Raji cells were opsonized in NHS  $\pm$  RTX  $\pm$  mAb 3E7 or were incubated in NHS with RTX and one of the other mAbs which bind to B cells (all final concentrations were  $10 \mu\text{g/mL}$ ). After 2 washes, cells were reconstituted in BSA-PBS containing  $2 \text{ mg/mL}$  mouse IgG and probed with Alexa 594 mAb 7C12 ( $10 \mu\text{g/mL}$ ). After 30 minutes' incubation at room temperature, cells were washed twice, transferred to a 96-well plate, and fluorescence intensities measured on a Wallac Victor II plate reader (Perkin Elmer, Gaithersburg, MD).

**Fluorescence microscopy.** Cells were incubated with 50% NHS and Alexa-labeled mAbs, washed, fixed in 1% paraformaldehyde in PBS, reconstituted to a concentration of about  $6 \times 10^6$  cells/mL, and examined with a BX40 fluorescent microscope (Olympus America, Melville, NY), equipped with either a PM20 camera or Magnafire digital camera (Olympus), using FITC, FITC/Texas Red, or Texas Red bandpass filters. Parallel experiments using unlabeled mAbs demonstrated that labeling of either RTX or mAb 3E7 with  $^{125}\text{I}$  or the fluorescent dyes did not affect their immunologic activities.

**Killing assays.** Cells were adjusted to about  $4 \times 10^5/\text{mL}$  in complete medium, and  $250 \mu\text{L}$  were mixed with  $250 \mu\text{L}$  of NHS or complete medium, followed by addition of RTX  $\pm$  mAb 3E7, or, in some of the experiments with DB cells,  $\pm$  one of the mAbs that also bind to B cells (see "Monoclonal antibodies"). Mixtures were incubated for varying periods at  $37^{\circ}\text{C}$  in 5%  $\text{CO}_2$ , and after 2 washes were stained with FITC annexin V and propidium iodide (PI) according to the manufacturer's directions (Caltag). In most cases  $50 \mu\text{L}$  (out of  $500 \mu\text{L}$  total) of stained cell suspension was counted, which was expected to give about 10 000 counts in samples in

which neither cell growth nor killing occurred. Forward and side scattering were used to identify the entire population of cells (including live, dead, and aggregated cells); debris generated as a consequence of cell lysis was excluded. Fluorescence analysis was performed with CellQuest software on a FACSCalibur flow cytometer (Becton Dickinson, San Jose, CA).

### Tests for binding of mAb 3E7 to normal cells

Aliquots of whole blood anticoagulated with citrate were incubated with FITC mAb 3E7  $\pm$  RTX, in the presence and absence of ARH-77 cells labeled with PKH26. After 30 minutes' incubation at  $37^{\circ}\text{C}$ , EDTA was added to a final concentration of  $0.01 \text{ M}$ , followed by APC-CD45 (Caltag). After 20 minutes' incubation at room temperature, erythrocytes were lysed with FACS-lyse (Becton Dickinson), cells were washed twice, reconstituted in PBS, and analyzed by flow cytometry. A standard gate of APC CD45 versus side scattering was used to identify basophils, granulocytes, monocytes, and lymphocytes, and binding of FITC mAb 3E7 was determined. Alternatively, cells in whole blood were washed and reconstituted in autologous serum  $\pm$  ARH-77 cells, and in addition to FITC mAb 3E7, Alexa 633 RTX was used in the opsonization step in order to identify CD20+ opsonized B cells, and samples were processed as described above, except PE-CD45 (Caltag) was used for gating.

### Studies in a monkey model

Two experiments were performed in cynomolgus monkeys (BL and NA), following protocols previously described.<sup>42,43</sup> Alexa (594 and 633) RTX and then Alexa 488 mAb 3E7 were infused intravenously into anesthetized animals. Blood samples were collected before and after each infusion, anticoagulated with EDTA and held on ice for processing within 30 minutes.

### Experiments with primary tumor cells

Blood samples were obtained with informed written consent from patients under treatment for CLL at the UVA Medical Center. Patient blood cells were washed twice and reconstituted in matched NHS as a C source,  $\pm 10 \mu\text{g/mL}$  RTX, and incubated up to 30 minutes at  $37^{\circ}\text{C}$ . The cells were washed twice and reconstituted in BSA-PBS containing  $2 \text{ mg/mL}$  mouse IgG and probed with Alexa mAbs HB43 and 3E7 to visualize bound RTX and C3b(i), respectively, by fluorescence microscopy. A similar protocol was followed in flow cytometry studies, except cells were also probed with PE antihuman IgM or PE anti-CD45, which along with the side scattering profile, allowed identification of B lymphocytes.

## Results

### Binding of RTX to CD20+ cells promotes C3b(i) deposition followed by binding of mAb 3E7

RTX binding to Raji cells in plasma-EDTA and in NHS was confirmed by indirect flow cytometry experiments using mAb HB43, specific for the Fc portion of human IgG (Figure 1; compare panels A,B with panels C,D). RTX binding to Raji cells in NHS, but not in plasma-EDTA, leads to robust complement activation and incorporation of substantial amounts of C3b(i) on the cells (Figure 1D). MAb 3E7 binds preferentially to an epitope on cell-bound C3b(i)<sup>5</sup> and this mAb can bind to cells in the presence of NHS or citrated plasma during complement opsonization. In fact, Alexa 488 mAb 3E7 binds to Raji cells during opsonization with Alexa 633 RTX in serum (compare panels E,F in Figure 1). The positive correlation in the dot plot suggests that those cells that bind the

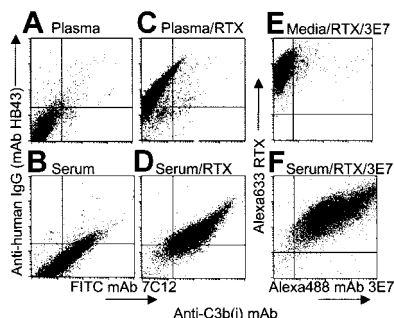


**Figure 1. RTX mediates deposition of C3b(i) on Raji cells in NHS.** (A-D) Cells were opsonized in 50% NHS (panels B,D) or in 50% plasma EDTA (panels A,C) ± RTX (10 µg/mL), and after 3 washes probed with a cocktail of FITC mAb 7C12 and PE mAb HB43. Panel D indicates that binding of RTX to cells in NHS leads to deposition of C3b(i). (E,F) Cells were opsonized with Alexa 633 RTX and Alexa 488 mAb 3E7 during incubation in complete medium (panel E) or in 50% NHS (panel F). Panel F reveals a positive correlation between binding of Alexa 633 RTX and Alexa 488 mAb 3E7 to Raji cells in NHS.

most RTX, and presumably activate complement and capture the most C3b(i), also bind the most mAb 3E7.

We used direct and indirect RIA to quantitate deposition of C3b(i) and binding of mAb 3E7 to Raji or ARH-77 cells when a variety of NHSs were used for C opsonization. The results in 50% NHS, summarized in Table 1, indicate that in the presence of both RTX and mAb 3E7, more than 1 million molecules of C3b(i) bind per Raji cell, and reduced but still substantial C opsonization occurs in the presence of either one of the mAbs alone. MAb 3E7 appears to facilitate a chain reaction in which binding of C3b to the cells leads to binding of mAb 3E7, which may either modestly activate C (mAb 3E7 is murine isotype IgG1) and/or enhance capture of additional molecules of C3b (Table 1; NHS vs NHS/mAb 3E7). RIA with <sup>125</sup>I-RTX revealed that 220 000 ± 43 000 molecules (n = 7) bound to Raji cells, and 310 000 ± 60 000 molecules (n = 4) bound to ARH-77 cells, in the presence and absence of C. We found that about 1 000 000 molecules of mAb 3E7 bind to the cells in the presence of RTX and C (Table 1). The

**Table 1. C3b(i) and mAb 3E7 bind to CD20+ cells during C/RTX opsonization**

Cells and incubation medium	Molecules bound per cell	
	C3b(i)*	Anti-C3b(i) mAb 3E7†
<b>Raji cells‡</b>		
NHS	300 000 ± 150 000   (18)	NA
NHS/RTX	610 000 ± 190 000 (18)	NA
NHS/RTX/mAb 3E7	1 400 000 ± 500 000 (13)	890 000 ± 220 000 (6)
NHS/mAb 3E7	680 000 ± 340 000 (14)	420 000 ± 190 000 (6)
<b>ARH-77 cells§</b>		
NHS	150 000 ± 60 000 (10)	NA
NHS/RTX	790 000 ± 230 000 (10)	NA
NHS/RTX/mAb 3E7	930 000 ± 240 000 (9)	1 100 000 ± 200 000 (3)
NHS/mAb 3E7	370 000 ± 110 000 (9)	240 000 ± 60 000 (3)

Values shown are averages ± SD. Numbers in parentheses indicate number of determinations. NA indicates not applicable.

\*Molecules bound were measured by indirect RIA based on probing with <sup>125</sup>I-anti-C3b(i) mAb 7C12.

†<sup>125</sup>I-anti-C3b(i) mAb 3E7 was used directly.

‡Either mAb singly or the combination gave more C3b(i) deposition than NHS alone ( $P < 10^{-3}$ ). RTX/mAb 3E7 gave more C3b(i) deposition than either mAb alone ( $P < 10^{-3}$ ). More mAb 3E7 was bound in the presence of RTX ( $P = 3 \times 10^{-3}$ ).

§Either mAb singly or the combination gave more C3b(i) deposition than NHS alone ( $P < 10^{-3}$ ). The combination gave more C3b(i) deposition than mAb 3E7 alone ( $P < 10^{-3}$ ). More mAb 3E7 was bound in the presence of RTX ( $P = 2 \times 10^{-3}$ ).

||Background level of binding of C3b(i) to the Raji (and ARH-77) cells in NHS has been previously reported.<sup>12,13</sup> Raji cells in NHS activate C, but less C3b(i) is bound than is observed in the presence of RTX.

results of steady state fluorescence measurements reveal that several other mAbs only modestly enhance RTX-mediated deposition of C3b(i) on Raji cells (Figure 2), and even lower levels of opsonization were obtained in the absence of RTX (not shown). However, use of the RTX/mAb 3E7 cocktail results in a significant increase in C3b(i) deposition.

**Colocalization of RTX and mAb 3E7**

We used fluorescence microscopy to address critical questions raised by the flow cytometry and RIA experiments concerning the molecular sites of binding of C3b(i) and mAb 3E7 to RTX-opsonized CD20+ cells in the presence of C. When Raji or ARH-77 cells were incubated with Alexa 594 RTX and Alexa 488 mAb 3E7 together in NHS or citrated plasma, the 2 mAbs colocalize on the cells (Figure 3A-C). In the presence of mAb 3E7 we often observe cross-linking of the cells, as well as capping and/or colocalization of the probes to discrete areas on the cells. If cells are opsonized with Alexa 594 RTX alone in citrated plasma, washed and then probed with Alexa 488 mAb 3E7, this mAb colocalizes with previously bound RTX, and in many cases cells are extensively cross-linked (Figure 3D). However, if FITC mAb HB43 is substituted for Alexa 488 mAb 3E7, mAb HB43 colocalizes with RTX, but no cross-linking is evident. Binding of RTX alone to cells in the presence or absence of NHS leads to a more homogenous binding pattern and neither capping nor cross-linking is observed (Figure 3E-F). A negative control experiment reveals that if cells are first reacted with mAb 3E7 in the presence of NHS and then washed and probed with RTX, the 2 probes bind to the cells with completely different patterns, and there is no evidence for colocalization (Figure 3G). Similar patterns of complement opsonization and colocalization of mAb 3E7 with RTX were demonstrable in DB cells (not shown).

**MAb 3E7 enhances RTX-mediated killing of Raji and DB cells**

C-mediated killing of nucleated cells requires multiple hits by the membrane attack complex (MAC) over an extended period,<sup>44</sup> and cells can recover by shedding the MAC. During this time the cells may continue to grow, and the new cells should also be subject to C attack. The relative rates of these processes can be variable, and therefore we have evaluated RTX-mediated killing by C over an extended period of time. In view of our observations of robust C activation and C3b(i) capture by Raji cells, we also sought to determine if combinations of C, RTX, and mAb 3E7 could kill these cells. Flow cytometry experiments (Figures 4; 5A-B) indicate that Raji cells grow in both complete medium and in NHS, and the rate of growth in medium containing RTX is lower than in medium

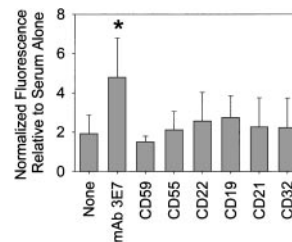


**Figure 2. MAb 3E7 enhances RTX-mediated deposition of C3b(i) on Raji cells.** Net steady state fluorescence intensity values, based on probing with Alexa 594 mAb 7C12, were normalized to 1 for treatment with each serum alone. The relative signal intensities for treatment with serum/RTX plus the noted additions (mAb 3E7 or mAbs specific for the epitopes indicated on the abscissa) are reported. The results for 8 different sera (duplicate determinations) were averaged. \* $P = 3 \times 10^{-3}$ .



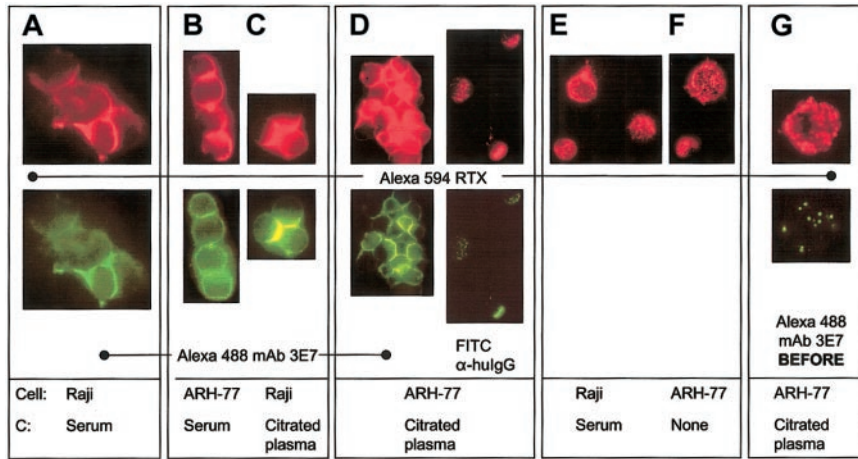


**Figure 3. Alexa 594 RTX and Alexa 488 mAb 3E7 colocalize on Raji and ARH-77 cells only if RTX is bound to the cells in the presence of a C source. (A-C)** Alexa 594 RTX and Alexa 488 mAb 3E7 colocalize on cells opsonized in NHS or in citrated plasma. Cross-linking and capping are evident. **(D)** After opsonization with RTX in citrated plasma, ARH-77 cells were washed and probed with either Alexa 488 mAb 3E7 or FITC  $\alpha$ -hulgG. **(E-F)** Alexa 594 RTX binds to cells in a homogeneous pattern if mAb 3E7 is omitted (panel E) or if NHS is omitted (panel F), and no cross-linking is observed. **(G)** When cells are opsonized in citrated plasma with Alexa 488 mAb 3E7, washed, and Alexa 594 RTX added, the probes do not colocalize, but they do colocalize when the order of addition is reversed (panel D). Original magnification  $\times$  250.

alone. We found that Raji cells are not effectively killed after a 1-hour incubation with RTX and C. Killing is, however, enhanced at longer times; incubation of the cells in NHS containing RTX leads to pronounced killing and suppression of growth by 24 to 48 hours.

In agreement with fluorescence microscopy experiments, some (about 50%) of the cells are cross-linked when they are incubated for 1 hour in NHS containing RTX + mAb 3E7. The arrow marked A in Figure 4 identifies the cross-linked population by its increase in forward and side scattering. This cross-linking is almost completely eliminated by 24 to 48 hours. As illustrated in Figures 4 and 5 and replicated in 30 independent experiments (Figure 6), use of mAb 3E7 in the presence of NHS and RTX enhances the action

of RTX and suppresses growth. MAb 3E7 by itself does not facilitate killing in NHS, and addition of mAb 3E7 to samples incubated in media  $\pm$  RTX had no effect on cell growth or killing (not shown). We also used another anti-CD20 mAb, 1F5, in these studies. This mAb was previously used in a phase 1 trial for B cell lymphoma therapy, although it is now known to promote cell growth.<sup>32,45,46</sup> We also observe substantial growth of cells in medium plus mAb 1F5; compared with medium alone, at 48 hours the number of live cells detected is reduced less than 2-fold (Figure 5A). Over 1 hour, mAb 1F5 kills Raji cells more effectively in NHS than does RTX, but as incubation times increase, the cells grow in mAb 1F5/NHS mixtures, while growth suppression and killing continue in the RTX/NHS mixtures (Figure 5B-D). The potential of

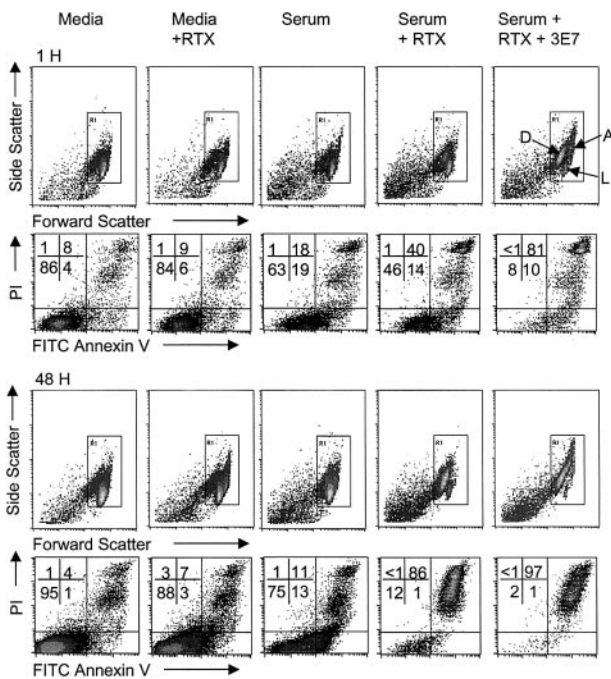


**Figure 4. Enhancement of RTX-mediated killing by mAb 3E7.** Raji cells in medium  $\pm$  RTX, or in 50% NHS  $\pm$  RTX  $\pm$  mAb 3E7 at 10  $\mu$ g/mL, were incubated for varying periods at 37°C in 5% CO<sub>2</sub> and stained with FITC annexin V and propidium iodide (PI). Forward and side scattering were used to identify the population of cells; debris generated as a consequence of cell lysis was excluded. Aggregated cells, live cells, and dead cells are indicated by arrows marked A, L, and D, respectively. The percentage of cells in each quadrant (live, lower left; dead, upper right) is displayed. The number of live cells at 1 hour and 48 hours for medium  $\pm$  RTX as well as for RTX  $\pm$  mAb 3E7 samples in serum is shown in Figure 5A-B.

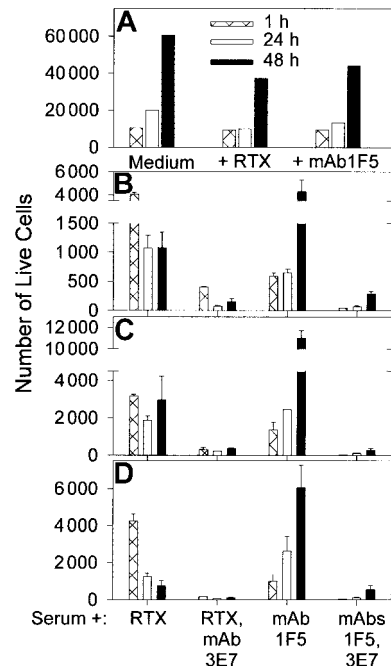


**Figure 5. Enhancement of RTX and mAb 1F5 C-mediated killing by mAb 3E7.** (A) Raji cells reacted with anti-CD20 mAbs RTX or 1F5 in complete medium show substantial growth after 48 hours of culture. (B-D) RTX and anti-CD20 mAb 1F5 mediate killing of Raji cells in 50% NHS, and mAb 3E7 enhances killing. Three different NHSs (O+, A+, B+) were tested in duplicate. Averages  $\pm$  SD are plotted. Total live cells were determined as described in the legend to Figure 4. By 48 hours, growth is evident in the mAb 1F5-treated samples, but mAb 3E7 suppresses growth in these samples.

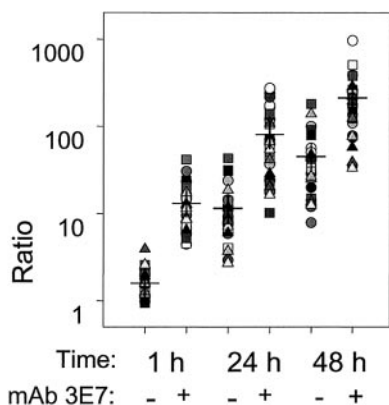


**Figure 6. Summary of 30 independent killing experiments for 15 different sera.** The ratio, the number of live Raji cells in NHS alone divided by the number of live cells for the treatment condition in NHS (RTX ± mAb 3E7), is displayed for individual NHSs at 3 different times. The means of the determinations are marked by horizontal dashes; the differences between RTX + mAb 3E7 vs RTX alone were statistically significant ( $P < 10^{-3}$ ) at all 3 times. The percentages of dead cells at 1 hour, 24 hours, and 48 hours for serum, serum + RTX, or serum + RTX + mAb 3E7 were as follows: 1 hour, 20 ± 10, 41 ± 12, 74 ± 11; 24 hours, 21 ± 14, 82 ± 12, 91 ± 7; 48 hours, 16 ± 11, 88 ± 9, 94 ± 5. For a given time the differences between the treatments were highly significant. In all cases  $P < 10^{-3}$  except for 48 hours, serum + RTX vs serum + RTX + mAb 3E7,  $P = 3 \times 10^{-3}$ .

mAb 1F5 to facilitate C-mediated killing and growth suppression is, however, substantially enhanced in the presence of mAb 3E7.

Raji cells at varying phases of growth from early to late log phase gave the same pattern of killing (not shown). The results of 30 independent experiments using our standard conditions (50% NHS, both RTX and mAb 3E7 at 10 µg/mL) are summarized in Figure 6. Effective killing of Raji cells in NHS by RTX is manifest after a 24-hour incubation period. Incorporation of mAb 3E7 in the incubation mixture enhances RTX-mediated killing as early as 1 hour, although part of this effect may be due to cross-linking (see Figures 3 and 4). Cross-linking is substantially reduced or eliminated after 24 to 48 hours, but enhanced killing and suppression of growth in the presence of RTX + mAb 3E7 are clearly evident.

We found that in complete medium RTX ± mAb 3E7 cannot promote killing of DB cells (Table 2). In addition, RTX is marginally effective at killing DB cells in NHS. We observed an approximate steady state; although killing is definitely demonstrable, new cells are generated at only a slightly lower rate than the rate at which cells are killed. However, in the presence of RTX + mAb 3E7 the steady state in 50% NHS shifts considerably to give more effective killing and growth suppression. Part of the reduction in live DB cells at 1 hour may be due to cross-linking, as noted previously in comparable experiments with Raji cells. By 48 hours, however, mAb 3E7 substantially enhances RTX-mediated killing and suppresses new cell growth (Table 2). As illustrated in Figure 7,

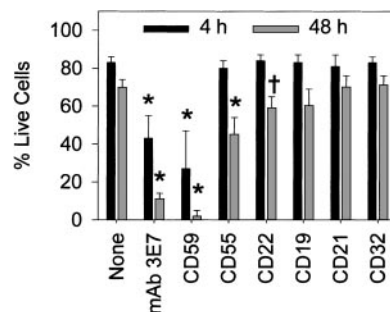


**Figure 7. Both mAb 3E7 and anti-CD59 enhance RTX-mediated killing of DB cells in serum.** Results (averages ± SD, 5 experiments) are reported for treatment with RTX/NHS plus the indicated additions (as described in the legend to Figure 2). In the absence of RTX, 90% of the cells were alive in serum at both 4 and 48 hours. \* $P < 10^{-3}$ ; † $P < 10^{-2}$  compared with RTX alone.

we extended the experiments on DB cell killing to include the panel of mAbs used in the steady state fluorescence measurements with Raji cells in Figure 2. The same pattern of simultaneous growth and killing of DB cells was observed in this experiment, and the percentage of live cells is reported. In agreement with the findings of Harjunpää et al<sup>31</sup> and Treon et al<sup>34</sup> in similar systems, neutralization of the activity of CD59 substantially increases RTX-mediated killing of DB cells in serum (Figure 7). Moreover, mAb 3E7 also significantly enhances killing; the other mAbs are far less effective. No killing was observed when the mAbs were used in the absence of RTX, and substitution of an isotype control for anti-CD59 did not enhance RTX-mediated killing (not shown).

**Complement is required for cell killing**

C-replete NHS is required for RTX killing; no killing of Raji cells is observed in heat-inactivated (C-depleted) NHS (not shown). C-mediated killing can continue over a prolonged period of time; after a 48-hour incubation at 37°C, CH 50 assays revealed that 50% of the initial complement activity is preserved in samples incubated with RTX ± mAb 3E7 (not shown). Effective C-mediated killing ultimately requires cell-mediated lysis by the MAC. ARH-77 cells express high levels of CD59<sup>34,47</sup> which blocks the action of the MAC, and are not lysed under the conditions of these experiments, even in the presence of mAb 3E7 and RTX. However, RTX can kill ARH-77 cells in the presence of baby rabbit C (BRC). At the 24 hour mark, incubation of ARH-77 cells with RTX in a 1:1 mixture of NHS and BRC led to 97% killing compared to incubation without RTX. Killing under these conditions presumably reflects the fact that human CD59 is less able to block the action of a MAC composed of rabbit C proteins.

**Table 2. MAb 3E7 enhances RTX-mediated killing of DB cells in NHS**

Condition	1 h			48 h		
	Live cells, no.	Live cells, %*	Dead cells, no.	Live cells, no.	Live cells, %*	Dead cells, no.
NHS	8700 ± 660	96 ± 0.2	190 ± 20	21 000 ± 900	94 ± 1	500 ± 30
NHS/RTX	8800 ± 250	72 ± 3	750 ± 200	7200 ± 1000	52 ± 5	5400 ± 700
NHS/RTX/mAb 3E7	1300 ± 180	36 ± 1	590 ± 140	700 ± 350	6 ± 3	8800 ± 600
Medium/RTX	5900 ± 400	88 ± 4	260 ± 30	22 500 ± 1200	86 ± 1	730 ± 80
Medium/RTX/mAb 3E7	6600 ± 470	91 ± 3	220 ± 20	21 500 ± 20	87 ± 0.1	650 ± 10

Values shown are averages ± SDs based on duplicate determinations with 3 different NHSs and are representative of 4 similar experiments. The NHS/RTX/mAb 3E7 sample had fewer live cells than NHS/RTX at both 1 hour and 48 hours ( $P < 10^{-3}$ ). More dead cells were present in the NHS/RTX/mAb 3E7 sample than in NHS/RTX at 48 hours ( $P < 10^{-3}$ ).

\*Percentage of live cells was calculated for each individual determination and then averaged.

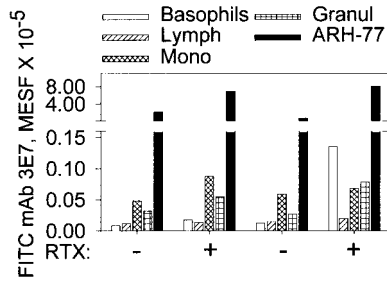


**Figure 8. mAb 3E7 binds weakly to normal cells in citrated whole blood compared with ARH-77 cells in the presence or absence of RTX.** The first 4 bars in each group represent FITC mAb 3E7 binding to blood cells from 2 healthy donors in the absence of ARH-77 cells; the fifth (black) bar denotes binding of FITC mAb 3E7 to PKH26-labeled ARH-77 cells added to whole blood. Binding of FITC mAb 3E7 to monocytes and granulocytes was 3000 to 8000 molecules of equivalent soluble fluorochrome (MESF); the isotype control averaged 2000. The slightly elevated binding of mAb 3E7 to basophils in the presence of RTX was not found in 4 other bloods (not shown). A standard gate of APC CD45 vs side scattering was used to identify basophils, granulocytes, monocytes, and lymphocytes. ARH-77 cells were identified based on the PKH26 label.

**Binding of mAb 3E7 to normal cells**

To be effective therapeutically, any mAb must show a high degree of specificity for malignant cells relative to normal cells. Due to the protective mechanisms of C control proteins, normal cells have low levels of C3b(i), and therefore direct binding of anti-C3b(i) mAbs should be minimal. However, immune complexes composed of mAb 3E7 and C3b(i) fragments generated in solution could bind to cells with C and/or Fc receptors. Based on flow cytometry determinations we observe weak binding of mAb 3E7 to normal cells in the presence of C ± RTX, but quantitatively there is far more binding to ARH-77 cells under these conditions (Figure 8). In a similar protocol we used FITC mAb 3E7 and Alexa 633 RTX to opsonize CD20-positive cells in washed whole bloods (± ARH-77 cells) reconstituted in NHS from 2 healthy donors. The MESF levels for binding of FITC mAb 3E7 to RTX-opsonized normal B cells, monocytes, granulocytes, and ARH-77 cells were, respectively, 38 000 ± 500, 17 500 ± 500, 16 000 ± 2000 and 250 000 ± 35 000 (n = 2), indicating that more mAb 3E7 binds to the RTX-opsonized malignant cells, presumably because they express higher levels of CD20. In NHS samples without either mAb, or in NHS-EDTA with both mAbs present, the background MESF values averaged 3000 for normal cells and 10 000 for ARH-77 cells. Finally, samples of diluted whole blood in NHS were cultured in the presence of mAb 3E7 (10 µg/mL) for 24 hours

and then probed with FITC-annexin V. We found no evidence for apoptosis of the cells after 24 hours; neither control samples nor the samples incubated with mAb 3E7 showed annexin V staining (not shown).

**Studies in a monkey model**

In vivo studies of C activation and C3b(i) capture were conducted by infusing Alexa 594/633 RTX into cynomolgus monkeys followed 10 or 20 minutes later by infusion of Alexa 488 mAb 3E7. A mixture of Alexa 594 and Alexa 633 RTX allows both fluorescence microscopy and flow cytometry measurements, respectively. Blood samples taken 2 minutes after infusion of RTX were washed and probed in vitro with Alexa mAb 3E7. Fluorescence microscopy revealed that cells which had bound RTX in vivo also took up mAb 3E7 in vitro (Figure 9A) and the fluorescence pattern is quite similar to that observed in in vitro experiments with Raji cells and ARH-77 cells (Figure 3A-C). That is, mAb 3E7 colocalizes with bound RTX on the cells, suggesting that C3b(i) rapidly deposits directly on cell-bound RTX in the circulation of the monkey. Parallel control experiments indicated mAb 3E7 did not bind to cells before RTX infusion (not shown). Samples B and C in Figure 9, taken after infusion of RTX followed by mAb 3E7, indicate that infused mAb 3E7 rapidly binds in vivo to RTX-opsonized cells; colocalization of the 2 mAbs is clearly evident.

Blood samples from the experiment with monkey BL were analyzed by flow cytometry (Figure 9D). Before infusion, naive B cells were positive for PE CD21 and negative for Alexa 633 RTX and Alexa 488 mAb 3E7 (plots 1-3). After Alexa 633 RTX infusion, a population of doubly positive CD21/RTX cells is apparent (plot 6). These cells also exhibit a small increase in the Alexa 488 mAb 3E7 and PE CD21 signal (plots 4-6), due to a compensation artifact. However, 1 minute after infusion of Alexa 488 mAb 3E7, the B cells show a large increase in the Alexa 488 mAb 3E7 signal (plots 7 and 8), which further demonstrates that mAb 3E7 rapidly binds to the RTX-opsonized cells in the circulation.

These experiments suggest that soon after infusion, RTX-opsonized B cells contain covalently associated C3b(i), and that mAb 3E7, at moderate concentrations, can rapidly bind to such opsonized cells via cell-associated C3b(i). C levels (CH50 assays) in the 2 animals before, during (1 hour after infusion of both mAbs), and 24 hours after the experiment were 492, 425, 506 and 62, 32, 28, respectively, thus suggesting that during the C3b

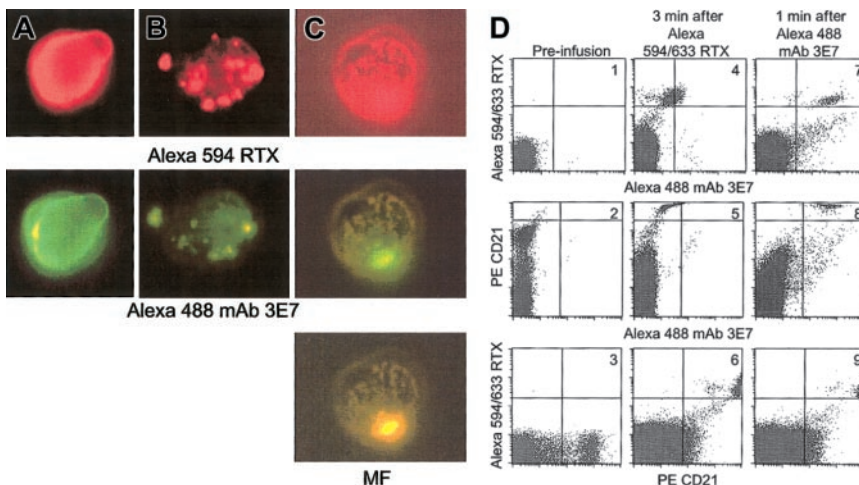


**Figure 9. RTX supports C3b deposition in a primate model.** Alexa 594/633 RTX was infused, followed 10 to 20 minutes later by Alexa 488 mAb 3E7. Blood samples were anticoagulated with EDTA, washed and probed as indicated. Erythrocytes were lysed and the remaining cells analyzed by fluorescence microscopy (panels A-C) or flow cytometry (panel D). Original magnification × 250. (A) Monkey BL: 2 minutes after Alexa 594/633 RTX (0.5 mg/kg) infusion, washed cells were probed with Alexa 488 mAb 3E7. (B) Ten minutes after infusion of Alexa 594/633 RTX and 2 minutes after infusion of Alexa 488 mAb 3E7 (1 mg/kg), cells were washed and examined without further probing. (C) Monkey NA: Treated as described in the legend to panel B, except 1.0 mg/kg Alexa 594/633 RTX. MF: mixed function filter. (D) Dot plots present the results of flow cytometry analyses of blood samples taken at different times during the experiment with monkey BL. PerCp CD45 and side scattering were used to identify lymphocytes, and the PE CD21 probe was used to identify B cells.



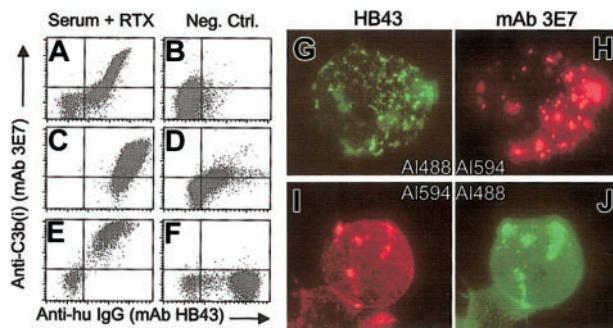


**Figure 10.** Addition of RTX to washed blood cells from CLL patients, reconstituted in NHS, leads to deposition of C3b(i). (A-F) The blood from 3 patients (panels A-B; C-D; E-F) was tested. Lymphocytes were identified based on PE CD45 and side scattering (panels A-B; E-F) or PE antihuman IgM and side scattering (panels C-D). The left panels (A,C,E) present the results of addition of RTX, followed by an incubation for 30 minutes (panels A,E) or 5 minutes (panel C) at 37°C. Samples were washed before probing. In panels B and D, RTX was omitted. In panel F, RTX was added to cells in serum-EDTA (to block C activation). (G-J) Samples from the third patient (panels E-F) were analyzed by fluorescence microscopy after probing with either AI488 HB43 and AI 594 mAb 3E7 (panels G-H) or Alexa 488 mAb HB43 and Alexa 488 mAb 3E7 (panels I-J). Both probing schemes reveal a substantial degree of colocalization of the probes. The Alexa 488 and Alexa 594 signals were visualized with the FITC and Texas Red filter, respectively. Original magnification  $\times 100$ .

opsonization process, there was some consumption of C in both animals. Although the C titer was low in the second monkey, it was adequate to facilitate C3b opsonization. Whether more C might be consumed in a human with a large tumor burden and a higher dose of RTX remains an open question. Aside from a decrease in lymphocytes and a temporary increase in neutrophils, there were no significant changes in the CBC profile, hepatic chemistry panel, or blood urea nitrogen during or 1 and 3 days after the experiment. In agreement with the studies of Reff et al, we found that after 1 hour more than 98% of the B cells (CD21<sup>+</sup>) were cleared from the circulation.<sup>28</sup>

#### Preliminary studies on blood obtained from patients with CLL

We performed in vitro experiments to test for RTX-mediated C3b(i) opsonization of CLL patient B cells. In order to ensure the reliability of the C source, matched NHS, previously titered for C activity, was used. The results of flow cytometry experiments indicate that in the presence of C, RTX facilitates rapid deposition of C3b(i) on CLL cells (Figure 10). Moreover, fluorescence micrographs, based on indirect probing for RTX and C3b(i), reveal marked colocalization of deposited C3b(i) with cell-bound RTX. These measurements serve as a prototype for the analysis of cell-bound RTX after it is infused into the bloodstream of a patient.

## Discussion

In view of the fact that only half of patients with non-Hodgkin lymphoma respond to RTX therapy,<sup>15-20</sup> attempts to increase the efficacy of this treatment require an understanding of its mechanism of action in vivo. Although there is uncertainty concerning this mechanism,<sup>21-37,48</sup> our results demonstrate that C plays an important role in RTX-mediated killing of Raji cells. Other mechanisms, such as growth arrest or apoptosis, do not facilitate substantial killing in the absence of C. Our findings agree with those of Ghetie et al, who demonstrated with several B-cell lymphoma lines, including Raji cells, that even when hyper-cross linking of CD20 is induced by use of RTX and an antihuman IgG reagent, the amount of killing/growth suppression is modest.<sup>23</sup>

Recently Bellosillo et al reported that incubation of malignant B cells in high concentrations of RTX induced absolutely no killing over 5 days in the absence of C.<sup>35</sup> Further clarification of the possible role of apoptosis in RTX-mediated killing in vivo<sup>27</sup> may be forthcoming in view of reports indicating that C activation on target cells may, under certain conditions, induce apoptosis.<sup>49</sup>

Neutralization of CD59 increased RTX-mediated killing of DB cells in serum (Figure 7), providing additional evidence supporting the role of C and the MAC in cell killing. The enhanced killing of Raji and DB cells promoted by mAb 3E7 in the presence of RTX and NHS is noteworthy (Figures 4-7; Table 2); aside from the anti-CD59 mAb, none of the other mAbs substantially enhanced RTX-mediated killing of DB cells, as was observed with mAb 3E7. We suggest that binding of mAb 3E7 to RTX-opsonized cells may increase C activation by either increasing capture of nascent C3b or by activating complement directly via an immune complex-mediated classical pathway mechanism. Capping and cross-linking due to binding of large amounts of mAb 3E7 (Figures 3-4) may cause disruptions and/or defects in the plasma membrane of the cell, which could prevent growth and lead to cell death. Such defects may also allow more effective attack by the MAC.

Evaluation of the mechanism(s) of action of RTX in vivo should consider the possible molecular forms of the molecule. We have demonstrated that large amounts of C3b(i) are deposited on CD20-positive cells in vitro in the presence of NHS and RTX in flow cytometry, RIA, and fluorescence microscopy experiments (Figures 1 and 3; Table 1). Based on evidence describing C3b(i) deposition on substrates during C activation,<sup>39,50-53</sup> C3b(i) is likely to be covalently bound to cell-bound RTX. The monkey model experiments (Figure 9) provide evidence that the C3b(i)-RTX complexes form in vivo; soon after RTX is infused, it promotes rapid complement activation and C3b(i) opsonization of monkey B cells. Moreover, in the circulation of the monkey, infused mAb 3E7 is able to bind to RTX-opsonized cells, presumably by binding to deposited C3b(i), and the fluorescence micrographs show the same patterns of colocalization that were manifest in the in vitro experiments with CD20-positive cell lines. These experiments, as well as our studies with blood samples from CLL patients (Figure 10), suggest that a similar pattern of complement activation and C3b(i) capture can occur when RTX is infused into humans.

The quantitative RIA (Table 1) indicate that 2 or more C3b(i) are cell-associated for each RTX IgG bound. A covalent complex of RTX and C3b(i) could interact with monocytes, macrophages and/or neutrophils via Fc and C receptors,<sup>2,6,47,54-56</sup> and the mechanism of action of RTX in vivo may include cell-mediated lysis and/or phagocytosis facilitated by these receptors. Recently Golay et al have reported in vitro experiments demonstrating that RTX enhances deposition of C3 on B cells isolated from 4 patients with B cell malignancies.<sup>36</sup>

ARH-77 cells were not killed by RTX + mAb 3E7 and C, indicating that up-regulation of C control proteins on cancer cells may block the action of immunotherapeutic modalities that require C activation and lysis by the MAC. Several studies suggest that up-regulation of these proteins may explain why lymphomas in some patients are refractory to the action of RTX.<sup>9,10,35,36</sup> However, Weng and Levy reported no correlation between the levels of C control proteins on patient cancer cells and therapeutic effectiveness of RTX in patients treated with RTX.<sup>48</sup> Moreover, they found no relationship between therapeutic effectiveness and the potential of RTX to facilitate C-mediated lysis of the respective cancer cells when NHS, but not autologous patient serum, was used as a C source.

We suggest an alternative mechanism to explain why RTX-mediated therapies may sometimes fail. Patients with cancer often have deficiencies in one or more proteins in the C pathway.<sup>57,58</sup> These deficiencies can be associated with inflammation induced by tumors and may represent the consequences of C consumption due to reaction of antibodies with tumors or circulating cancer cells. It is also possible that continued treatment with a tumor-specific mAb may consume sufficient C that the mAb's effectiveness will be compromised. Recently Byrd et al reported that treatment of CLL patients with high doses of RTX at an accelerated schedule led to some clinical benefit.<sup>14,27</sup> We note that this therapeutic regimen led to decreases in CH50 and C3 levels.<sup>14</sup> In fact, C levels in these patients were relatively low before treatment was initiated. It is possible that if the C activity of a patient with B cell lymphoma is low or reduced after prolonged treatment,<sup>14,27</sup> RTX might not provide maximally effective therapy. Immunotherapy with C-fixing mAbs may, therefore, be more effective if accompanied by in vitro testing to determine whether the patient's C level is adequate to support the intended action of the therapeutic mAb.<sup>59</sup> If in vitro tests reveal a deficiency in one or more C proteins it would be reasonable to treat the patient by infusion with either C replete plasma or with the C proteins found to be deficient. We note that relatively low C levels were sufficient to facilitate C3b(i) deposition on RTX-opsonized cells in the bloodstream of one of the

monkeys, and therefore the definition of "adequate" with respect to the effector functions of C remains uncertain.

In summary, we have demonstrated that binding of the anti-CD20 mAb RTX to Raji and ARH-77 cells in NHS leads to C activation and deposition of large amounts of C3b(i). Experiments in a monkey model, as well as in vitro studies with blood from CLL patients, extend and generalize these observations. Use of the anti-C3b(i)-specific mAb 3E7 in conjunction with RTX enhances both deposition of C3b(i) on Raji and ARH-77 cells and C-mediated killing of Raji and DB cells. If C activation is indeed the major route of therapeutic efficacy for RTX treatment, it may be important to increase the C activity in certain patients to realize the full therapeutic potential of RTX. Use of mAbs specific for C3b(i), such as mAb 3E7, and treatment of patients with plasma or C components may be reasonable approaches for enhancing the therapeutic efficacy of antitumor mAbs whose chief mechanism of action involves C-mediated killing.

## Acknowledgments

We thank C. Hess, J. Densmore, C. Teeple-Paully, and D. Rexrode for providing patient blood samples. This paper is dedicated to the loving memory of Peter Andrew Kollman.

## References

- Walport MJ. Complement. *N Engl J Med*. 2001; 344:1058-1066.
- Morgan BP, Harris CL. The complement system: a brief overview. In: Morgan BP, Harris CL, eds. *Complement Regulatory Proteins*. San Diego, CA: Academic Press; 1999:1-31.
- Volanakis JE. Overview of the complement system. In: Volanakis JE, Frank MM, eds. *The Human Complement System in Health and Disease*. New York, NY: Marcel Dekker Inc; 1998:9-32.
- Lambris JD, Sahu A, Wetsel RA. The chemistry and biology of C3, C4 and C5. In: Volanakis JE, Frank MM, eds. *The Human Complement System in Health and Disease*. New York, NY: Marcel Dekker Inc; 1998:83-119.
- Sokoloff MH, Nardin A, Solga MD, et al. Targeting of cancer cells with monoclonal antibodies specific for C3b(i). *Cancer Immunol Immunother*. 2000;49:551-562.
- Ross GD, Vetvicka V, Yan J, Xia Y, Vetvickova J. Therapeutic intervention with complement and  $\beta$ -glucan in cancer. *Immunopharmacology*. 1999; 42:61-74.
- Irie K, Irie RF, Morton DL. Evidence for in vivo reaction of antibody and complement to surface antigens of human cancer cells. *Science*. 1974; 186:454-456.
- Vetvicka V, Thornton BP, Ross GD. Soluble  $\beta$ -glucan polysaccharide binding to the lectin site of neutrophil or natural killer cell complement receptor type 3 (CD11b/CD18) generates a primed state of the receptor capable of mediating cytotoxicity of iC3b-opsonized target cells. *J Clin Invest*. 1996;98:50-61.
- Gorter A, Meri S. Immune evasion of tumor cells using membrane-bound complement regulatory proteins. *Immunol Today*. 1999;20:576-582.
- Juriansz K, Ziegler S, Garcia-Schuler H, et al. Complement resistance of tumor cells: basal and induced mechanisms. *Mol Immunol*. 1999;36: 929-939.
- Springer GF. Immunoreactive T and Tn epitopes in cancer diagnosis, prognosis, and immunotherapy. *J Mol Med*. 1997;75:594-602.
- Olesen EH, Johnson AA, Damgaard G, Leslie RGQ. The requirement of localized, CR2-mediated, alternative pathway activation of complement for covalent deposition of C3 fragments on normal B cells. *Immunology*. 1998;93:177-183.
- Schwendinger M, Spruth M, Schoch J, Dierich M, Proding W. A novel mechanism of alternative pathway complement activation accounts for the deposition of C3 fragments on CR2-expressing homologous cells. *J Immunol*. 1997;158:5455-5463.
- Byrd J, Murphy T, Howard R, et al. Rituximab using a thrice weekly dosing schedule in B-cell chronic lymphocytic leukemia and small lymphocytic lymphoma demonstrates clinical activity and acceptable toxicity. *J Clin Oncol*. 2001;19:2153-2164.
- Coiffier B, Haioun C, Ketterer N, et al. Rituximab (anti-CD20 monoclonal antibody) for the treatment of patients with relapsing or refractory aggressive lymphoma: a multicenter phase II study. *Blood*. 1998;92:1927-1932.
- Colombat P, Salles G, Brousse N, et al. Rituximab (anti-CD20 monoclonal antibody) as single first-line therapy for patients with follicular lymphoma with a low tumor burden: clinical and molecular evaluation. *Blood*. 2001;97:101-106.
- Grillo-Lopez A, White C, Varns C, et al. Overview of the clinical development of rituximab: first monoclonal antibody approved for the treatment of lymphoma. *Semin Oncol*. 1999;26:66-73.
- Czuczman MS, Grillo-Lopez A, Saleh W, et al. Treatment of patients with low-grade B-cell lymphoma with the combination of chimeric anti-CD20 monoclonal antibody and CHOP chemotherapy. *Clin Oncol*. 1999;17:268-276.
- Maloney DG, Grillo-Lopez AJ, White CA, et al. IDEC-C2B8 (Rituximab) anti-CD20 monoclonal antibody therapy in patients with relapsed low-grade non-Hodgkin's lymphoma. *Blood*. 1997;90: 2188-2195.
- McLaughlin P, Grillo-Lopez AJ, Link BK, et al. Rituximab chimeric anti-CD20 monoclonal antibody therapy for relapsed indolent lymphoma: half of patients respond to a four-dose treatment program. *J Clin Oncol*. 1998;16:2825-2833.
- Clynes RA, Towers TL, Presta LG, Ravetch JV. Inhibitory Fc receptors modulate in vivo cytotoxicity against tumor targets. *Nat Med*. 2000;6:443-446.
- Gopal AK, Press OW. Clinical applications of anti-CD20 antibodies. *J Lab Clin Med*. 1999;134:445-450.
- Ghetie M, Bright H, Vitetta E. Homodimers but not monomers of Rituxan (chimeric anti-CD20) induce apoptosis in human B-lymphoma cells and synergize with a chemotherapeutic agent and an immunotoxin. *Blood*. 2001;97:1392-1398.
- Shan D, Ledbetter J, Press O. Signaling events involved in anti-CD20-induced apoptosis of malignant human B cells. *Cancer Immunol Immunother*. 2000;48:673-683.
- Shan D, Ledbetter JA, Press OW. Apoptosis of malignant human B cells by ligation of CD20 with monoclonal antibodies. *Blood*. 1998;91:1644-1652.
- Cartron G, Dacheux L, Salles G, et al. Therapeutic activity of humanized anti-CD20 monoclonal antibody and polymorphism in IgG Fc receptor Fc $\gamma$ RIIa gene. *Blood*. 2002;99:754-758.
- Byrd JC, Kitada S, Flinn IW, et al. The mechanism of tumor cell clearance by rituximab in vivo in patients with B-cell chronic lymphocytic leukemia: evidence of caspase activation and apoptosis induction. *Blood*. 2002;99:1038-1043.
- Reff ME, Carner K, Chambers KS, et al. Depletion of B cells in vivo by a chimeric mouse human monoclonal antibody to CD20. *Blood*. 1994;83: 435-445.
- Idusogie EE, Presta LG, Gazzano-Santoro H, et al. Mapping of the C1q binding site on Rituxan, a chimeric antibody with a human IgG1 Fc. *J Immunol*. 2000;164:4178-4184.
- Idusogie EE, Wong PY, Presta LG, et al. Engineered antibodies with increased activity to recruit complement. *J Immunol*. 2001;166:2571-2575.
- Harjunpää A, Junnikkala S, Meri S. Rituximab (anti-CD20) therapy of B-cell lymphomas: direct complement killing is superior to cellular effector mechanisms. *Scand J Immunol*. 2000;51:634-641.
- Golay J, Zaffaroni L, Vaccari T, et al. Biologic response of B lymphoma cells to anti-CD20 monoclonal antibody rituximab in vitro: CD55 and



- CD59 regulate complement mediated cell lysis. *Blood*. 2000;95:3900-3908.
33. Flieger D, Renoth S, Beier I, Sauerbrunch T, Schmidt-Wolf I. Mechanism of cytotoxicity induced by chimeric mouse human monoclonal antibody IDEC-C2B8 in CD20-expressing lymphoma cell lines. *Cell Immunol*. 2000;204:55-63.
  34. Treon S, Mistsiades C, Mistsiades N, et al. Tumor cell expression of CD59 is associated with resistance to CD20 serotherapy in patients with B-cell malignancies. *J Immunother*. 2001;24:263-271.
  35. Bellosillo B, Villamor N, Lopez-Guillermo A, et al. Complement-mediated cell death induced by rituximab in B-cell lymphoproliferative disorders is mediated in vitro by a caspase-independent mechanism involving the generation of reactive oxygen species. *Blood*. 2001;98:2771-2777.
  36. Golay J, Lazzari M, Facchinetti V, et al. CD20 levels determine the in vitro susceptibility to rituximab and complement of B-cell chronic lymphocytic leukemia: further regulation by CD55 and CD59. *Blood*. 2001;98:3383-3389.
  37. van der Kolk LE, Grillo-Lopez AJ, Baars JW, Hack CE, Van Oers MHJ. Complement activations plays a key role in the side-effects of rituximab treatment. *Br J Haematol*. 2001;115:807-811.
  38. Tomic L, Sutherland WM, Kurek J, Edberg JC, Taylor RP. Preparation of monoclonal antibodies to C3b by immunization with C3b(i)-sepharose. *J Immunol Methods*. 1989;120:241-249.
  39. Edberg JC, Tomic L, Wright EL, Sutherland WM, Taylor RP. Quantitative analyses of the relationship between C3 consumption, C3b capture, and immune adherence of complement-fixing antibody/DNA immune complexes. *J Immunol*. 1988;141:4258-4265.
  40. Fraker PJ, Speck JC. Protein and cell membrane iodinations with a sparingly soluble chloroamide, 1,3,4,6-tetrachloro-3a,6a-diphenylglycol uril. *Biochem Biophys Res Commun*. 1978;80:849-857.
  41. Harlow E, Lane D. *Antibodies: A Laboratory Manual*. Cold Spring Harbor, NY: Cold Spring Harbor Laboratory; 1988:354-355.
  42. Lindorfer MA, Hahn CS, Foley PL, Taylor RP. Heteropolymer-mediated clearance of immune complexes via erythrocyte CR1: mechanisms and applications. *Immunol Rev*. 2001;183:10-24.
  43. Craig ML, Reinagel ML, Martin EN, et al. Infusion of bispecific monoclonal antibody complexes into monkeys provides immunologic protection against later challenge with a model pathogen. *Clin Immunol*. 1999;92:170-180.
  44. Morgan BP. Complement membrane attack on nucleated cells: resistance, recovery and non-lethal effects. *Biochem J*. 1989;264:1-14.
  45. Press O, Appelbaum F, Ledbetter J, et al. Monoclonal antibody 1F5 (anti-CD20) serotherapy of human B cell lymphomas. *Blood*. 1987;69:584-591.
  46. Deans JP, Robbins SM, Polyak MJ, Savage JA. Rapid redistribution of CD20 to a low density detergent-insoluble membrane compartment. *J Biol Chem*. 1998;273:344-348.
  47. Stockmeyer B, Dechant M, van Egmond M, et al. Triggering Fc $\alpha$ -receptor I (CD89) recruits neutrophils as effector cells for CD20-directed antibody therapy. *J Immunol*. 2000;165:5954-5961.
  48. Weng WK, Levy R. Expression of complement inhibitors CD46, CD55, and CD59 on tumor cells does not predict clinical outcome after rituximab treatment in follicular non-Hodgkin lymphoma. *Blood*. 2001;98:1352-1357.
  49. Fishelson Z, Attali G, Mevorach D. Complement and apoptosis. *Mol Immunol*. 2001;38:207-219.
  50. Gadd KJ, Reid KB. The binding of complement component C3 to antibody-antigen aggregates after activation of the alternative pathway in human serum. *Biochem J*. 1981;195:471-480.
  51. Brown EJ, Joiner KA, Gaither TA, Hammer CH, Frank MM. The interaction of C3b bound to *Pneumococci* with factor H (beta 1H globulin), factor I (C3b/C4b inactivator), and properdin factor B of the human complement system. *J Immunol*. 1983;131:409-415.
  52. Vidarte L, Pastor C, Mas S, et al. Serine 132 is the C3 covalent attachment point on the CH1 domain of human IgG1. *J Biol Chem*. 2001;276:38217-38223.
  53. Shohet J, Bergamaschini L, Davis A, Caroll M. Localization of the human complement C3 binding site on the IgG heavy chain. *J Biol Chem*. 1991;266:18520-18524.
  54. Fries LF, Siwik SA, Malbran A, Frank MM. Phagocytosis of target particles bearing C3b-IgG covalent complexes by human monocytes and polymorphonuclear leucocytes. *Immunology*. 1987;62:45-51.
  55. Gaither TA, Vargas I, Inada S, Frank MM. The complement fragment C3d facilitates phagocytosis by monocytes. *Immunology*. 1987;62:405-411.
  56. Wallace PK, Valone FH, Fanger MW. Myeloid cell-targeted cytotoxicity of tumor cells. In: Fanger MW, ed. *Bispecific Antibodies*. Austin, TX: R. G. Landis Co; 1995:43-76.
  57. Lugassy G, Platok I, Schlesinger M. Hypocomplementemia in multiple myeloma. *Leuk Lymphoma*. 1999;33:365-370.
  58. Schlesinger M, Broman I, Lugassy G. The complement system is defective in chronic lymphatic patients and in healthy relatives. *Leukemia*. 1996;10:1509-13.
  59. Brezicka T, Einbeigi Z, Bergman B. Functional assessment in vitro of human-complement-dependent antibody-induced cytotoxicity of neoplastic cells. *Cancer Immunol Immunother*. 2000;49:235-242.